

# SVFit: Parameter-Efficient Fine-Tuning of Large Pre-Trained Models Using Singular Values

Chengwei Sun, Jiwei Wei\*, Yujia Wu, Yiming Shi, Shiyuan He, Zeyu Ma, Ning Xie, and Yang Yang

**Abstract**—Large pre-trained models (LPMs) have demonstrated exceptional performance in diverse natural language processing and computer vision tasks. However, fully fine-tuning these models poses substantial memory challenges, particularly in resource-constrained environments. Parameter-efficient fine-tuning (PEFT) methods, such as LoRA, mitigate this issue by adjusting only a small subset of parameters. Nevertheless, these methods typically employ random initialization for low-rank matrices, which can lead to inefficiencies in gradient descent and diminished generalizability due to suboptimal starting points. To address these limitations, we propose SVFit, a novel PEFT approach that leverages singular value decomposition (SVD) to initialize low-rank matrices using critical singular values as trainable parameters. Specifically, SVFit performs SVD on the pre-trained weight matrix to obtain the best rank- $r$  approximation matrix, emphasizing the most critical singular values that capture over 99% of the matrix's information. These top- $r$  singular values are then used as trainable parameters to scale the fundamental subspaces of the matrix, facilitating rapid domain adaptation. Extensive experiments across various pre-trained models in natural language understanding, text-to-image generation, and image classification tasks reveal that SVFit outperforms LoRA while requiring 16 times fewer trainable parameters.

**Index Terms**—Large pre-trained model, parameter-efficient fine-tuning, singular values.

## I. INTRODUCTION

ARGE pre-trained models (LPMs), such as RoBERTa [1] with an impressive 125 million trainable parameters, ViT [2] boasting 354 million parameters, and LLaMA [3] featuring 700 million to 65 billion parameters, have become indispensable tools in natural language processing [4]–[6] and computer vision [7]–[13], showcasing remarkable performance across a spectrum of tasks. The industry's relentless pursuit of scaling up model parameters to the billion or even trillion range continues to push the boundaries of large models [14]–[16]. Nonetheless, the immense size and computational demands of these models present significant challenges for adapting them to specific downstream tasks, particularly in resource-constrained environments [17], [18].

In response to this challenge, parameter-efficient fine-tuning (PEFT) methods have emerged as a promising solution to reduce memory requirements [19]–[24]. These methods focus on updating a limited subset of parameters—either a portion of

the existing model parameters or an entirely new set [25]–[27]. The main goal is to retain the knowledge embedded in LPMs while adapting them to specific tasks, thereby minimizing the risk of catastrophic forgetting. Among these methods, Low-Rank Adaptation (LoRA) [19] has garnered particular attention for its stable performance across diverse downstream tasks. LoRA is based on the hypothesis that LPMs can still learn effectively when projected onto a smaller subspace due to the low intrinsic dimensionality of the tasks [28]. It introduces two low-rank matrices,  $A$  and  $B$ , to approximate weight updates during fine-tuning. Specifically, LoRA initializes  $A$  using a Gaussian distribution and sets  $B$  to zero, as illustrated in Fig. 2(a). This initialization scheme enables incremental updates to be seamlessly integrated into the pre-trained weights without causing significant delays in inference. Building on LoRA's foundation, several subsequent approaches [20], [21], [23], [29] have adhered to this paradigm, experimenting with various initialization strategies such as Kaiming uniform [30], and further enhance computational efficiency. However, this raises the question of whether random initialization is indeed optimal. Specifically, random initialization may prevent the main components of the pre-trained weight matrix  $W$  from being effectively updated during the initial stages of fine-tuning. This limitation could lead to inefficiencies in gradient descent, potentially resulting in suboptimal local minima and impairing the generalization performance of the model.

This paper introduces SVFit, an innovative PEFT strategy for LPMs. SVFit utilizes a distinctive initialization strategy by applying SVD to the pre-trained weight matrix  $W$ , resulting in two components: the best rank- $r$  approximation matrix  $W_r$  and a residual matrix  $W_e$ , with  $W_e$  capturing the smaller singular values. Our analysis verifies that the top 10%, or even 1%, of singular values contribute to over 99% of the total matrix sum. As depicted in Fig. 1, SVD was performed on the Fishstar, with the first set of experiments arranging the singular values in descending order and reconstructing the images using the largest 8, 16, 32, 64, 128, and 256 singular values, as shown in the first row. The second set of experiments arranged the singular values in ascending order, reconstructing the images with the smallest 8, 16, 32, 64, 128, and 256 singular values, with results displayed in the second row. These findings underscore the critical role of larger singular values in preserving image quality. Therefore, the pre-trained weight matrix  $W$  can be effectively approximated using only the most significant singular values above a threshold  $r$ , while the smaller singular values contribute minimally to the overall structure. As a result,  $W_r$  retains the essential pre-trained knowledge, and  $W_e$  is kept frozen during training. Addition-

\*Corresponding author

Chengwei Sun, Jiwei Wei, Yujia Wu, Yiming Shi, Shiyuan He, Zeyu Ma, Ning Xie, and Yang Yang are with the Center for Future Media and School of Computer Science and Engineering, University of Electronic Science and Technology of China, Chengdu 611731, China (e-mail: suncw10@126.com; mathematic6@gmail.com; 202322080314@std.uestc.edu.cn; yiming-shi666@gmail.com; shiyuanhe.david@gmail.com; cnzeyuma@163.com; seanxiening@gmail.com; yang.yang@uestc.edu.cn).

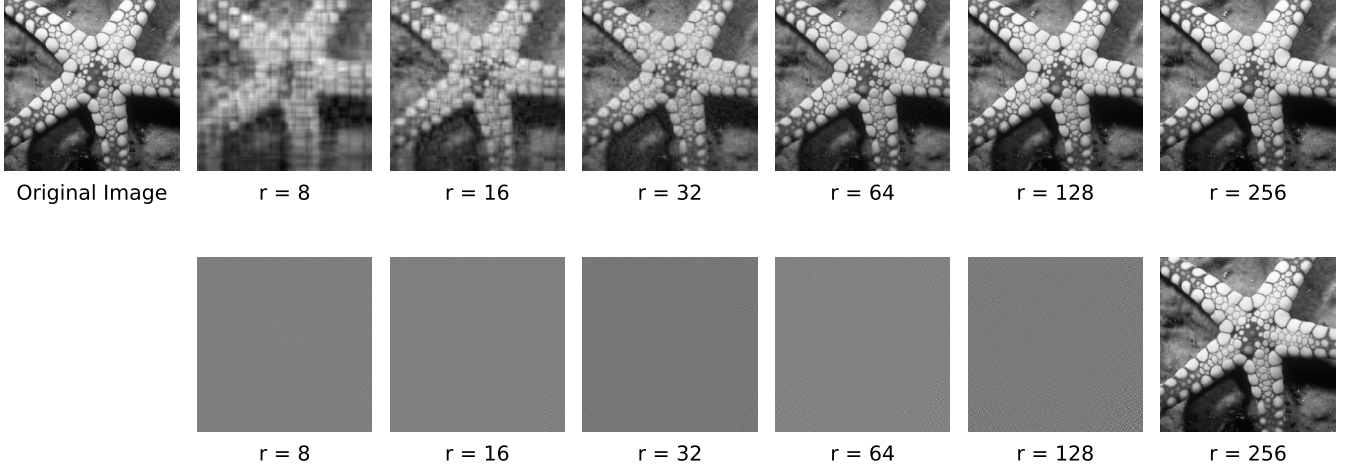


Fig. 1. SVD-based reconstruction results of the Fishstar image ( $256 \times 256$ ) [31]. The first row shows the reconstruction using the top 8, 16, 32, 64, 128, and 256 largest singular values, sorted in descending order ( $r = 8, r = 16, r = 32, r = 64, r = 128, r = 256$ ). The second row displays the reconstruction using the smallest 8, 16, 32, 64, 128, and 256 singular values, sorted in ascending order. This comparison highlights the pivotal role of dominant singular values in maintaining image quality, while the smallest singular values have minimal impact on the overall structure.

ally, inspired by recent advances in image generation that demonstrate the effectiveness of learnable scaling factors for improved domain adaptation [32], SVFit uses the most critical singular values obtained from SVD as trainable parameters. Only the top  $r$  singular values  $\Sigma_r$  within  $W_r$  are trained, with the fundamental subspaces derived from SVD scaled to promote rapid adaptation to new domains, as illustrated in Fig. 2(c) and Fig. 3. This approach enhances the learning of new domain knowledge for downstream tasks while preserving pre-trained information and significantly reducing the number of trainable parameters.

Extensive experiments have been conducted to verify the effectiveness of SVFit across various tasks and models. Specifically, RoBERTa-base and RoBERTa-large were used for natural language understanding tasks, ViT-base and ViT-large were used for image classification tasks, and Stable Diffusion v1.5 was used for subject-driven text-to-image task. The experimental results demonstrate that SVFit achieves superior performance with a significantly reduced number of parameters. For instance, in the image classification task using the ViT-large model, SVFit outperforms LoRA with only 0.036M trainable parameters, compared to LoRA's 0.8M.

The primary contributions of this paper are as follows:

- We present SVFit, a novel PEFT method that enhances the initialization process by utilizing SVD to initialize low-rank matrices derived from pre-trained weights. SVFit focuses on training only the most significant top- $r$  singular values, significantly reducing the number of trainable parameters while achieving efficient fine-tuning and preserving the model's core capabilities.
- We offer a theoretical analysis to uncover the mechanisms underlying SVFit. This analysis demonstrates how leveraging singular values enables rapid adaptation by effectively capturing the essential information from pre-trained models and efficiently learning new domain-specific knowledge with minimal parameters.
- SVFit is evaluated on a range of tasks, such as natural lan-

guage understanding, image classification, and subject-driven text-to-image generation. It consistently outperforms LoRA and other recent state-of-the-art techniques in terms of parameter efficiency and overall performance.

## II. RELATED WORK

### A. Parameter-Efficient Fine-Tuning

With the development of LPMs, adapting models with billions of parameters to specific downstream tasks has become increasingly challenging due to their complexity and computational demands [33]–[36]. Parameter-efficient fine-tuning (PEFT) has garnered significant attention in recent years for its ability to minimize the parameters and memory requirements needed while maintaining efficiency and accuracy, achieving performance comparable to full fine-tuning. Certain PEFT methods achieve fine-tuning by incorporating supplementary modules or optimizing prompts and prefixes. For instance, Adapter [37] integrates lightweight trainable parameters between pre-trained layers while maintaining fixed pre-trained weights. Prefix tuning [26] involves appending prefix parameters to the hidden states across all layers of the model. Prompt tuning [27] utilizes templates to reconstruct prompts, updating only parameters relevant to prompt comprehension. Despite their significant performance gains, these approaches unavoidably introduce additional overhead during inference.

### B. Low-Rank Adaptation

Low-Rank Adaptation (LoRA) [19] introduces two low-rank matrices to approximate weight updates during fine-tuning, seamlessly integrating incremental updates into pre-trained weights without causing noticeable delays in inference. To be specific, when provided with a pre-trained weight matrix  $W \in \mathbb{R}^{d_1 \times d_2}$ , after full fine-tuning on a specific domain task, the new weight matrix is  $W + W'$ , where  $W'$  represents the update containing domain knowledge. LoRA is designed to

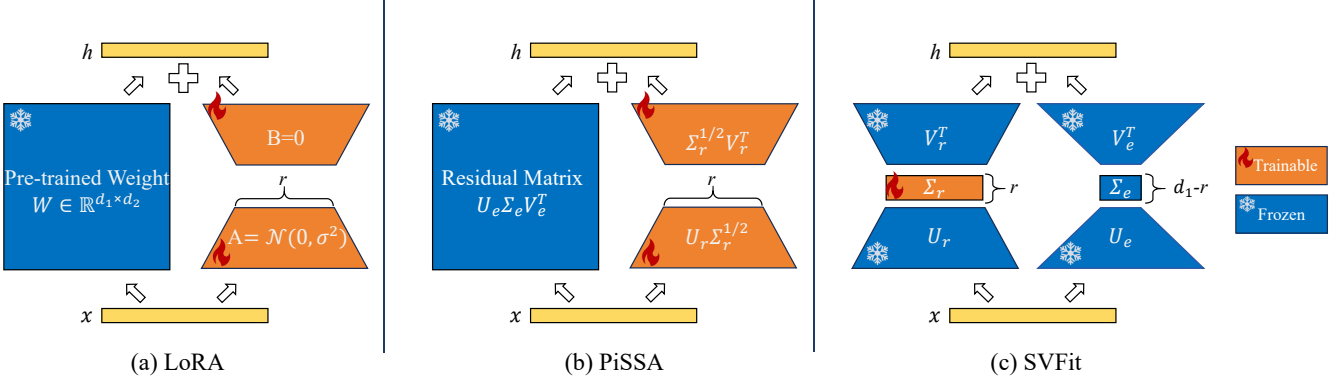


Fig. 2. Visual comparison among LoRA, PiSSA, and SVFit. (a) LoRA introduces two low-rank matrices  $A$  and  $B$  to approximate weight updates during fine-tuning. (b) PiSSA initializes  $A$  and  $B$  with the principal components of the pre-trained weight  $W$ , freezing the residual matrix during fine-tuning. (c) SVFit initializes low-rank matrices through SVD of  $W$  and trains only the most significant top- $r$  singular values (for simplicity,  $d_1 \ll d_2$  is assumed).

progressively update  $W'$  and break down  $W'$  through the matrix multiplication of two low-rank matrices  $A$  and  $B$ ,

$$W' = AB, \quad (1)$$

where  $A \in \mathbb{R}^{d_1 \times r}$ , and  $B \in \mathbb{R}^{r \times d_2}$  with intrinsic rank  $r \ll \min(d_1, d_2)$ . For  $h = Wx$ , the modified computation of the forward pass can be represented as

$$h = (W + W')x = (W + AB)x. \quad (2)$$

In the initial training phase,  $A$  undergoes random Gaussian initialization, while  $B$  is initialized to zeros, as shown in Fig. 2(a). This method freezes  $W$  and specifically updates  $A$  and  $B$ , significantly reducing the number of trainable parameters for downstream tasks compared to full fine-tuning. Additionally, LoRA integrates the values of matrices  $A$  and  $B$  into  $W$  during the inference phase, ensuring that this adaptation does not introduce additional delays.

### C. LoRA's Variants

Building upon LoRA, several studies have proposed modifying the parameter update strategy. LoRA-FA [29] freezes the low-rank matrix  $A$  within LoRA, significantly reducing trainable parameters and activation memory costs without increasing computational overhead. Delta-LoRA [20] updates both low-rank matrices  $A$  and  $B$ , propagating these changes to the pre-trained weight  $W$  using the delta of their product. PiSSA [38] initializes  $A$  and  $B$  with the principal components of the original matrix  $W$  and places the remaining components into a residual matrix, which is kept frozen during fine-tuning. Another strategy to improve LoRA is to allow for the adaptable adjustment of LoRA rank. AdaLoRA [39] utilizes SVD to parameterize incremental updates and dynamically distributes the parameter budget among weight matrices based on their importance score. SORA [40] employs an optimizable gate with a proximal gradient method to control sparsity, expanding the optimization space and improving parameter efficiency. Similarly, Zhang et al. [41] suggest IncreLoRA, an incremental parameter allocation method that adaptively incorporates trainable parameters during training according to the importance scores of each module.

## III. METHOD

In this section, we present SVFit, a novel PEFT approach for LPMs that leverages singular values for improved model adaptation. Unlike conventional methods that preserve the knowledge of LPMs by freezing the pre-trained weight matrix  $W$ , SVFit aims to embed this knowledge into low-rank matrices and retain it permanently. SVFit achieves this by performing SVD on the pre-trained weight matrix  $W$ , using the most critical singular values as trainable parameters, thereby optimizing the initialization of low-rank matrices for more effective fine-tuning.

### A. Fundamental Subspaces Derived from SVD

We begin by introducing key concepts related to Singular Value Decomposition (SVD) and fundamental subspaces, a technique widely used in pattern recognition and data compression [42], [43]. SVD transforms a dataset from a high-dimensional space to a lower-dimensional space by ranking the singular values according to their significance [44], [45]. Dimensionality reduction is achieved by discarding the less significant singular values, while the remaining singular values, when combined with their corresponding singular vectors, define the reduced-dimensional space.

**Definition 1** (Range space). *Given a matrix  $W \in \mathbb{R}^{d_1 \times d_2}$ , the range space of matrix  $W$  is the vector space spanned by the columns of  $W$ . In other words, the range space is the set of all possible linear combinations of the column vectors of  $W$ . The range space is often denoted as  $\mathbf{R}(W)$ . Formally, the range space is defined as:*

$$\mathbf{R}(W) = \{Wx \mid x \in \mathbb{R}^{d_2}\} \subseteq \mathbb{R}^{d_1}. \quad (3)$$

*Similarly, the range space of  $W^T$  is a subspace of  $\mathbb{R}^{d_2}$ , denoted as  $\mathbf{R}(W^T)$ . That is,*

$$\mathbf{R}(W^T) = \{W^Ty \mid y \in \mathbb{R}^{d_1}\} \subseteq \mathbb{R}^{d_2}. \quad (4)$$

**Definition 2** (Null space). *Given a matrix  $W \in \mathbb{R}^{d_1 \times d_2}$ , the null space of matrix  $W$  is the set of all vectors  $x \in \mathbb{R}^{d_2}$  that are mapped to the zero vector in  $\mathbb{R}^{d_1}$  when multiplied by  $W$ . Formally, the null space is defined as:*

$$\mathbf{N}(W) = \{x \mid Wx = 0\} \subseteq \mathbb{R}^{d_2}. \quad (5)$$

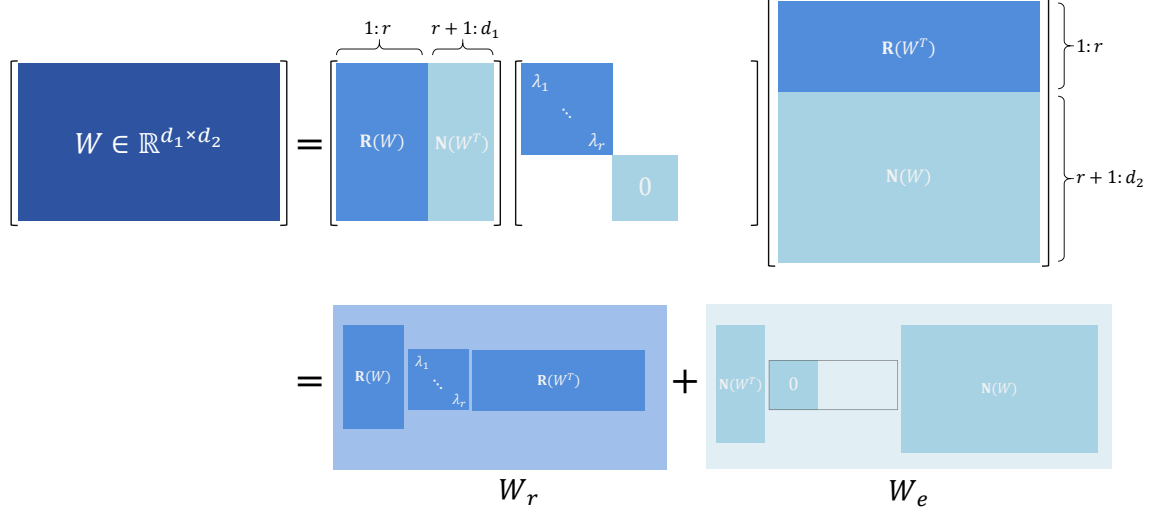


Fig. 3. Illustration of the SVD of matrix  $W$  and its fundamental subspaces: This figure illustrates the SVD of the pre-trained weight matrix  $W \in \mathbb{R}^{d_1 \times d_2}$ , where  $W$  is decomposed into singular values and vectors as  $W = U \text{diag}(\Sigma) V^T$ . The decomposition yields a rank- $r$  approximation matrix  $W_r$  and a residual matrix  $W_e$ . Specifically, the range space of  $W$  is spanned by  $U_r$ , and its null space is spanned by  $V_e$ . Conversely, the range space of  $W^T$  is spanned by  $V_r$ , and its null space is spanned by  $U_e$ .

Similarly, the null space of matrix  $W^T$  consists of all vectors  $y \in \mathbb{R}^{d_1}$  that are mapped to the zero vector in  $\mathbb{R}^{d_2}$  when multiplied by  $W^T$ . The formal definition of the null space of  $W^T$  is as follows:

$$\mathbf{N}(W^T) = \{y \mid W^T y = 0\} \subseteq \mathbb{R}^{d_1}. \quad (6)$$

Given a matrix  $W \in \mathbb{R}^{d_1 \times d_2}$  of rank  $r$ , its SVD is denoted as  $W = U \text{diag}(\Sigma) V^T$ , where  $\text{diag}(\Sigma)$  is a  $d_1 \times d_2$  diagonal matrix containing the singular values  $\{\lambda_i\}_{1 \leq i \leq r}$  of  $W$  in descending order, with  $r \ll \min(d_1, d_2)$ . The matrices  $U = [u_1, u_2, \dots, u_{d_1}] \in \mathbb{R}^{d_1 \times d_1}$  and  $V = [v_1, v_2, \dots, v_{d_2}] \in \mathbb{R}^{d_2 \times d_2}$  are orthogonal matrices. We can partition  $U$  and  $V$  into two parts by columns and denote these partitions as  $U_r$ ,  $U_e$ , and  $V_r$ ,  $V_e$ , respectively:

$$U_r = [u_1, u_2, \dots, u_r], U_e = [u_{r+1}, u_{r+2}, \dots, u_{d_1}], \quad (7)$$

$$V_r = [v_1, v_2, \dots, v_r], V_e = [v_{r+1}, v_{r+2}, \dots, v_{d_2}]. \quad (8)$$

Then the four fundamental subspaces associated with matrix  $W$  can be obtained:

- $U_r$  is the orthonormal basis for the range space of  $W$ , i.e.,  $\mathbf{R}(U_r) = \mathbf{R}(W)$ ;
- $U_e$  is the orthonormal basis for the null space of  $W^T$ , i.e.,  $\mathbf{R}(U_e) = \mathbf{N}(W^T)$ ;
- $V_r$  is the orthonormal basis for the range space of  $W^T$ , i.e.,  $\mathbf{R}(V_r) = \mathbf{R}(W^T)$ ;
- $V_e$  is the orthonormal basis for the null space of  $W$ , i.e.,  $\mathbf{R}(V_e) = \mathbf{N}(W)$ .

To verify that  $\mathbf{R}(V_e) = \mathbf{N}(W)$ , one would show that the subspace spanned by  $V_e$  consists precisely of the vectors that  $W$  maps to the zero vector. Similar arguments can be applied to verify the other subspaces.

*Proof.* Assume the rank of the matrix  $W \in \mathbb{R}^{d_1 \times d_2}$  is  $r$  and  $d_1 \ll d_2$ . Thus, the singular values are ordered as  $\lambda_1 \geq \lambda_2 \geq \dots \geq \lambda_r > \lambda_{r+1} = \dots = \lambda_{d_1} = 0$ .

Since  $W = U \text{diag}(\Sigma) V^T = \sum_{i=1}^r \lambda_i u_i v_i^T$ , we can express  $W$  as  $Wx = \sum_{i=1}^r \lambda_i u_i v_i^T x$ . Let  $z = \sum_{i=r+1}^{d_2} \beta_i v_i$ , then  $Wz = (\sum_{i=1}^r \lambda_i u_i v_i^T) (\sum_{i=r+1}^{d_2} \beta_i v_i) = 0$ . Therefore, the null space of  $W$  is  $\mathbf{N}(W) = \{x \mid Wx = 0\} = \mathbf{R}(V_e)$ .  $\square$

The connection between the SVD of the matrix  $W$  and the four fundamental subspaces can be depicted in Fig. 3.

### B. SVFit: PEFT of LPMs Using Singular Values

SVFit performs SVD on the initial pre-trained weight matrix  $W \in \mathbb{R}^{d_1 \times d_2}$  within the self-attention and multilayer perceptron layers to obtain the best rank- $r$  approximation

$$W_r = U_r \text{diag}(\Sigma_r) V_r^T, \quad (9)$$

and the residual matrix

$$W_e = U_e \text{diag}(\Sigma_e) V_e^T, \quad (10)$$

where  $U_r = [u_1, u_2, \dots, u_r] \in \mathbb{R}^{d_1 \times r}$  and  $V_r = [v_1, v_2, \dots, v_r] \in \mathbb{R}^{d_2 \times r}$  are the matrices of singular vectors corresponding to the top  $r$  singular values, and  $U_e = [u_{r+1}, u_{r+2}, \dots, u_{d_1}] \in \mathbb{R}^{d_1 \times (d_1-r)}$  and  $V_e = [v_{r+1}, v_{r+2}, \dots, v_{d_2}] \in \mathbb{R}^{d_2 \times (d_2-r)}$  are the matrices of singular vectors corresponding to the residual singular values. As discussed in Section III-A,  $\mathbf{R}(U_r) = \mathbf{R}(W)$ ,  $\mathbf{R}(V_r) = \mathbf{R}(W^T)$ ,  $\mathbf{R}(U_e) = \mathbf{N}(W^T)$ , and  $\mathbf{R}(V_e) = \mathbf{N}(W)$ . The singular values are arranged in descending order, with  $\Sigma_r = [\lambda_1, \lambda_2, \dots, \lambda_r]$  and  $\Sigma_e = [\lambda_{r+1}, \lambda_{r+2}, \dots, \lambda_{d_1}]$ . Consequently, the pre-trained weight matrix  $W$  can be expressed as:

$$\begin{aligned} W &= W_r + W_e = U_r \text{diag}(\Sigma_r) V_r^T + U_e \text{diag}(\Sigma_e) V_e^T \\ &= \sum_{i=1}^r \lambda_i u_i v_i^T + \sum_{i=r+1}^{d_1} \lambda_i u_i v_i^T, \end{aligned} \quad (11)$$

as shown in Fig. 2(c) and Fig. 3.

As observed in Fig. 1, we performed SVD on the Fishstar to reconstruct images using various subsets of singular values: the top 8, 16, 32, 64, 128, and 256 singular values, as well as the smallest 8, 16, 32, 64, 128, and 256 singular values. The results highlight that larger singular values are crucial for preserving image quality. Notably, the top 10% or even 1% of singular values contribute to over 99% of the total matrix sum. This observation indicates that the pre-trained weight matrix  $W$  can be effectively approximated by focusing on the most significant singular values above a given threshold  $r$ , while the smaller singular values have minimal impact on the overall structure. Consequently, in SVFit,  $W_e$  is frozen during training, and the focus is placed on adapting  $W_r$ . Inspired by recent advancements in image generation, such as learnable scaling factors for improved domain adaptation [32], SVFit utilizes the most critical singular values obtained from SVD as the trainable parameters. Specifically, it trains only the top  $r$  singular values  $\Sigma_r$  in  $W_r$ , while scaling the fundamental subspace derived from SVD to facilitate rapid adaptation to new domains. In a word, the matrices  $U_r$ ,  $V_r$ ,  $U_e$ ,  $V_e$ , and  $\Sigma_e$  are kept frozen, and the training focuses exclusively on the most significant top- $r$  singular values  $\Sigma_r$ , as demonstrated in Fig. 2(c) and Fig. 3. This method allows features to be projected onto a low-rank subspace defined by the orthogonal columns of  $U$  and  $V$ , enabling efficient layer-wise adaptation with a reduced number of trainable parameters.

In comparison to other LoRA variants, SVFit uniquely employs the most critical singular values from SVD initialization as trainable parameters, leading to more effective learning of new domain knowledge for downstream tasks while preserving pre-trained information. This approach significantly reduces the number of trainable parameters without introducing additional computational overhead or latency during inference, as the module can be seamlessly integrated into the original matrix post-training.

#### IV. EXPERIMENT

In this section, we conduct extensive experiments to evaluate SVFit in the contexts of natural language understanding and computer vision. We fine-tune the RoBERTa-base and RoBERTa-large models [1] on the GLUE benchmark [46] and apply SVFit to fine-tune ViT-base and ViT-large models [2] for image classification tasks [47], [48]. Additionally, we fine-tune Stable Diffusion v1.5 [49] to generate diverse images of a subject instance in various environments [50], [51]. We also vary the rank in our method for one task to examine how performance scales with the number of trainable parameters and analyze the influence of the learning rate. Our experiments are conducted using PyTorch, with pre-trained weights and configuration files obtained from HuggingFace [52], on NVIDIA A6000 GPUs.

##### A. Baselines

We compare SVFit with full fine-tuning and popular PEFT methods, including LoRA, DyLoRA, AdaLoRA, and PiSSA.

- Full fine-tuning involves updating the entire set of model parameters, initialized with pre-trained weights and biases, through gradient descent [53]. Although this approach is straightforward and robust, it demands substantial computational resources.
- LoRA [19] employs two low-rank matrices to learn incremental updates, reducing GPU memory cost. We replicate their experimental setup for a fair comparison.
- DyLoRA [24] dynamically selects a random rank  $r$  for LoRA modules during training.
- AdaLoRA [39] addresses the challenge of optimal rank selection for incremental updates by adaptively pruning singular values based on their magnitudes, resulting in different ranks for different layers.
- PiSSA [38], structurally similar to LoRA, initializes the adapter matrices  $A$  and  $B$  using the principal components of the original weight matrix  $W$ , while the remaining components form a residual matrix that is kept frozen during fine-tuning.

TABLE I  
HYPERPARAMETER SETUP OF SVFIT FOR THE GLUE BENCHMARK

	Hyperparameter	COLA	STS-B	RTE	MRPC	SST-2	QNLI
Base	Rank				768		
	Warmup Ratio				0.06		
	LR Scheduler				Linear		
	Weight Decay				0.1		
	Trainable Matrices				$W_Q, W_V$		
	Max Sequence Length				512		
	Epochs	80	40	80	30	60	25
	Batch Size	64	64	16	64	64	64
Large	Learning Rate	0.01	0.01	0.01	0.02	0.003	0.003
	Rank				768		
	Batch Size				32		
	Warmup Ratio				0.06		
	LR Scheduler				Linear		
	Weight Decay				0.1		
	Trainable Matrices				$W_Q, W_V$		
	Max Sequence Length				128		
Large	Epochs	40	20	40	40	10	20
	Learning Rate	0.01	0.01	0.01	0.003	0.001	0.002

##### B. Natural Language Understanding

**Models and Datasets.** We evaluate our method on the GLUE benchmark (General Language Understanding Evaluation). This comprehensive natural language understanding assessment encompasses various tasks, including sentence relationship recognition, sentiment analysis, and natural language reasoning [46]. For systematic evaluation, we select six tasks: CoLA [54], STS-B [55], RTE [56], MRPC [57], SST-2 [58], and QNLI [59]. We implement SVFit for fine-tuning RoBERTa-base, which has 12 layers with a hidden size of 768, totaling 125 million parameters, and RoBERTa-large, which has 24 layers with a hidden size of 1024, totaling 356 million parameters [1].

**Implementation Details.** For all six datasets in GLUE, we tune the hyperparameters for learning rates and scaling values. Following the experimental setup used in previous studies [19], [20], we fine-tune only the query and value weights in each transformer block while fully fine-tuning the classification

TABLE II

PERFORMANCE COMPARISON OF VARIOUS FINE-TUNING METHODS ON THE GLUE BENCHMARK USING ROBERTA-BASE AND ROBERTA-LARGE MODELS. METRICS INCLUDE MCC FOR COLA, PCC FOR STS-B, AND ACC FOR RTE, MRPC, SST-2, AND QNLI. RESULTS ARE REPORTED AS THE MEDIAN OF 5 RUNS WITH DIFFERENT RANDOM SEEDS. THE HIGHEST SCORE FOR EACH DATASET IS HIGHLIGHTED IN BOLD, WITH HIGHER VALUES INDICATING BETTER PERFORMANCE ACROSS ALL METRICS

	Method	# Trainable Parameters	CoLA (MCC)	STS-B (PCC)	RTE (ACC)	MRPC (ACC)	SST-2 (ACC)	QNLI (ACC)	Avg.
Base	FT	125M	63.6	91.2	78.7	<b>90.2</b>	94.8	92.8	<b>85.2</b>
	LoRA	0.3M	63.4	91.5	78.4	89.7	<b>95.1</b>	<b>93.3</b>	<b>85.2</b>
	DyLoRA	0.3M	61.1	91.1	78.7	89.5	94.3	92.2	84.5
	AdaLoRA	0.3M	62	90.5	<b>81</b>	88.7	94.5	93.1	85.0
	PiSSA	0.3M	63.8	90.8	75.5	89.2	94.7	92.5	84.4
Large	SVFit	<b>0.018M</b>	<b>64.8</b>	<b>92.4</b>	78.0	90.0	94.4	90.8	85.1
	FT	356M	68	92.4	86.6	90.9	96.4	94.7	88.2
	LoRA	0.8M	68.2	92.3	85.2	90.2	96.2	94.8	87.8
	PiSSA	0.8M	69.0	<b>92.9</b>	85.2	90.2	<b>96.7</b>	<b>95.1</b>	88.2
	SVFit	<b>0.036M</b>	<b>71.4</b>	92.0	<b>86.3</b>	<b>90.9</b>	96.2	94.4	<b>88.5</b>

TABLE III

PERFORMANCE COMPARISON OF VARIOUS FINE-TUNING METHODS ON THE IMAGE CLASSIFICATION TASK USING ViT-BASE AND ViT-LARGE MODELS ACROSS DIFFERENT DATASETS. ACCURACY (%) IS REPORTED AFTER TEN EPOCHS. AVG. REPRESENTS THE AVERAGE ACCURACY ACROSS ALL DATASETS. THE BEST PERFORMANCE FOR EACH DATASET IS HIGHLIGHTED IN BOLD

	Method	# Trainable Parameters	OxfordPets	CIFAR10	DTD	EuroSAT	RESISC45	StanfordCars	FGVC	CIFAR100	Avg.
Base	Head	-	90.3	96.4	69.8	88.7	74.2	25.8	17.4	84.3	68.4
	FT	85.8M	93.1	<b>98.9</b>	77.7	<b>99.1</b>	<b>96.1</b>	79.8	<b>54.8</b>	<b>92.4</b>	<b>86.5</b>
	LoRA	0.3M	93.2	98.8	75.0	98.4	92.7	45.4	25.2	92.0	77.6
	PiSSA	0.3M	95.9	98.6	78.7	98.7	95.5	67.1	47.6	91.2	84.2
	SVFit	<b>0.018M</b>	<b>97.0</b>	98.8	<b>80.5</b>	98.6	93.0	67.2	47.9	91.6	84.3
Large	Head	-	91.1	97.8	73.3	92.6	82.0	37.9	24.6	84.3	73.0
	FT	303.3M	94.4	99.2	81.8	<b>99.0</b>	<b>96.4</b>	<b>88.9</b>	<b>68.3</b>	93.6	<b>90.2</b>
	LoRA	0.8M	94.8	99.1	81.8	98.6	94.7	73.3	42.3	<b>94.9</b>	84.9
	PiSSA	0.8M	96.7	98.8	77.8	98.8	95.7	86.7	62.6	92.6	88.7
	SVFit	<b>0.036M</b>	<b>97.8</b>	<b>99.3</b>	<b>83.4</b>	98.7	95.2	83.3	57.8	93.9	88.7

TABLE IV  
HYPERPARAMETER SETUP FOR IMAGE CLASSIFICATION OF SVFIT

Hyperparameter	OxfordPets	CIFAR10	DTD	EuroSAT	
Base	Rank	768			
	Epochs	10			
	LR Scheduler	Linear			
	Weight Decay	0.01			
	Trainable Matrices	$W_Q, W_V$			
Large	Learning Rate	0.04	0.04	0.04	0.2
	Rank	768			
	Epochs	10			
	LR Scheduler	Linear			
	Weight Decay	0.01			
Base	Trainable Matrices	$W_Q, W_V$			
	Learning Rate	0.06	0.03	0.03	0.1
Hyperparameter	RESISC45	StanfordCars	FGVC	CIFAR100	
Base	Rank	768			
	Epochs	10			
	LR Scheduler	Linear			
	Weight Decay	0.01			
	Trainable Matrices	$W_Q, W_V$			
Large	Learning Rate	0.2	0.4	0.2	0.04
	Rank	768			
	Epochs	10			
	LR Scheduler	Linear			
	Weight Decay	0.01			
	Trainable Matrices	$W_Q, W_V$			
	Learning Rate	0.07	0.4	0.3	0.1

head. For both models, the rank of LoRA is set to 8, and the rank of SVFit is set to 768. Due to time constraints and budget limitations, we omit the time-intensive MNLI and QQP tasks, thereby forgoing the MNLI trick for MRPC, RTE, and

STS-B tasks. Consistent with prior work [21], [60], we report the number of trainable parameters in the fine-tuned layers, explicitly excluding the classification head, which is trained in a standard way. The results are averaged over five different random seeds. Additional details are provided in Table I.

**Results.** Based on the results presented in Table II, our proposed SVFit method demonstrates superior performance in several key areas compared to both traditional fine-tuning (FT) and other PEFT methods such as LoRA, DyLoRA, AdaLoRA, and PiSSA. For RoBERTa-base, SVFit achieves the highest Matthew’s correlation coefficient (MCC) for CoLA and the highest Pearson correlation coefficient (PCC) for STS-B, indicating its effectiveness in classification and regression tasks. While it falls slightly behind in accuracy (ACC) for MRPC and SST-2, it maintains competitive performance across all tasks, resulting in a robust overall average. For RoBERTa-large, SVFit outperforms other methods on CoLA, RTE, and MRPC and achieves comparable performance on other tasks. Its significant improvement in MCC for CoLA is noteworthy, reflecting its strength in complex language understanding tasks. The results suggest that SVFit’s approach to fine-tuning, with its unique parameterization and efficient use of trainable parameters, offers a balanced and effective alternative to existing methods. Additionally, the method’s reduced number of trainable parameters demonstrates its potential for achieving high performance with lower computational costs.

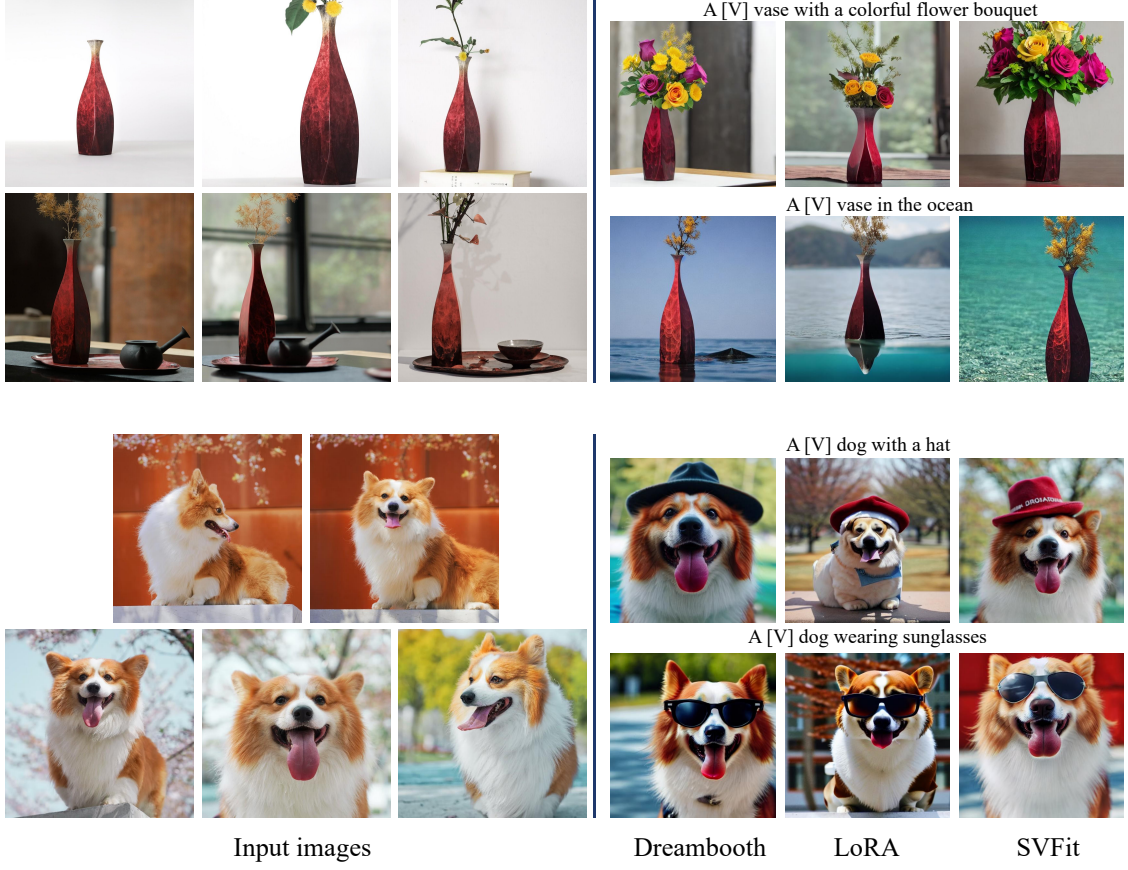


Fig. 4. Randomly selected samples from DreamBooth, LoRA, and SVFit for the subject-driven generation task.

### C. Image Classification

**Models and Datasets.** We assess SVFit on the image classification task using both the base and large versions of the widely adopted Vision Transformer (ViT) model [2], pre-trained on the ImageNet-21K dataset [61]. To ensure a comprehensive evaluation, we employ a diverse set of datasets, including OxfordPets [62], CIFAR10 [63], DTD [64], EuroSAT [65], RESISC45 [66], StanfordCars [67], FGVC [68], and CIFAR100 [63].

**Implementation Details.** We evaluated the performance of LoRA, PiSSA, and SVFit applied to the query and value layers of the ViT, in addition to two baseline approaches: full fine-tuning (FT) and training only the classification head (referred to as Head). Consistent with our GLUE benchmark setup, the rank of LoRA is set to 8 and the rank of SVFit to 768 for both models. Learning rates were meticulously tuned for all methods, with the maximum training epoch limited to 10. The reported parameter counts exclude the classification head, which is trained across all methods. Further details are provided in Table IV.

**Results.** Table III illustrates the performance of various fine-tuning methods on image classification tasks using ViT-base and ViT-large models across various datasets. Notably, our proposed SVFit method demonstrates strong performance with both model sizes. For the ViT-base, SVFit achieves the highest accuracy on OxfordPets (97.0%) and DTD (80.5%)

and performs competitively on other datasets, resulting in an overall average accuracy of 84.3%. While FT achieves the highest average accuracy (86.5%), it requires significantly more trainable parameters (85.8M) compared to SVFit's minimal 0.018M parameters. For ViT-large, SVFit again stands out by achieving the highest accuracy on OxfordPets (97.8%), CIFAR10 (99.3%), DTD (83.4%), and performs well across other datasets with an average accuracy of 88.7%. FT still yields the highest average accuracy (90.2%) but at the cost of training 303.3M parameters, whereas SVFit uses only 0.036M parameters. These results underscore the efficiency and effectiveness of SVFit, particularly in scenarios where computational resources and parameter efficiency are critical. By maintaining competitive performance while dramatically reducing the number of trainable parameters, SVFit offers a compelling alternative to traditional fine-tuning methods.

### D. Dreambooth

**Models and Datasets.** Following [51], we evaluate our method on the subject-driven text-to-image generation task. By fine-tuning Stable Diffusion v1.5 [49] using DreamBooth, we can generate diverse images of a subject instance in various environments, maintaining high preservation of subject details and realistic interactions between the scene and the subject. We compare our approach with LoRA and DreamBooth [51], ensuring fairness by randomly selecting generated images from

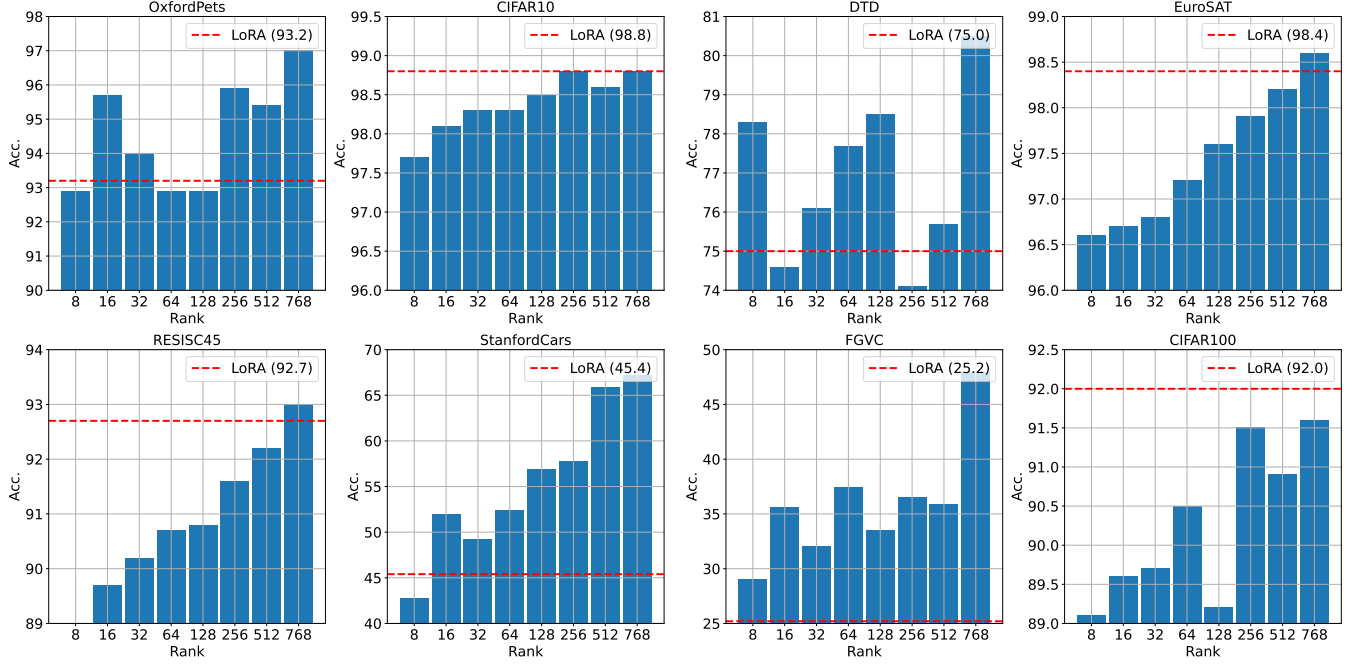


Fig. 5. Performance of SVFit fine-tuning for ViT-base model on image classification tasks across different parameter budget levels. The  $x$ -axis represents the rank, and the  $y$ -axis is the evaluation index of different datasets.

both methods. For fine-tuning, we use the dataset introduced in DreamBooth [51], which includes five or six images per subject for training.

**Implementation Details.** Both LoRA and our method use the same loss function as in DreamBooth. For DreamBooth and LoRA, we apply the best hyperparameter setup in the original paper [51].

**Results.** In Fig. 4, we present a comparative analysis of image generation using Dreambooth, LoRA, and SVFit across multiple scenarios. SVFit consistently demonstrates superior subject detail preservation and context integration. For instance, in the "vase with a colorful flower bouquet" scenario, SVFit accurately retains the intricate details of the flowers and vase while seamlessly blending them with the background. In contrast, the results from Dreambooth and LoRA exhibit noticeable artifacts and inconsistencies in subject representation and background interaction. Overall, the visual comparison clearly illustrates SVFit's enhanced capability in generating high-fidelity images that closely follow the given prompts, effectively preserving subject details and ensuring realistic environmental interactions.

#### E. Different Budget Levels

We analyzed the performance of SVFit fine-tuning on the ViT-base model for image classification tasks under different parameter budget levels. The specific results are shown in Fig. 5. We employed various ranks  $r = \{8, 16, 32, 64, 128, 256, 512, 768\}$ , corresponding to 0.2K, 0.4K, 0.8K, 1.5K, 3.1K, 6.1K, 12.3K, and 18.4K trainable parameters, respectively. For LoRA, we used a baseline rank of  $r = 8$ , corresponding to 294.9K trainable parameters. The experimental results demonstrate that our method effectively

balances the number of trainable parameters and accuracy. For instance, on the OxfordPets dataset, our method achieves an accuracy of approximately 93.2% at the lowest rank of 8 while maintaining or improving accuracy with higher ranks. Similarly, for the CIFAR10 dataset, our method achieves an accuracy of around 98.8% at rank 8, with further gains observed as the rank increases. This trend is consistent across other datasets. Our method significantly improves over the baseline across various datasets and rank levels, maintaining high performance with fewer trainable parameters.

#### F. Analysis of Learning Rate

Adjusting the learning rate is a crucial step in fine-tuning. Our method requires a larger learning rate than LoRA since our initialization strategy has already initialized most of the model's parameters to a certain extent, and a larger learning rate can help quickly adapt the remaining parameters to the new tasks. We perform a learning rate search using our method, as shown in Fig. 6. A learning rate 10 $\times$  greater than pre-training yields the best results across multiple datasets. For instance, on the OxfordPets dataset, the accuracy peaks at approximately 93.2% with a 10 $\times$  learning rate, while both lower (0.5 $\times$ , 1 $\times$ , 5 $\times$ ) and higher learning rates (50 $\times$ , 100 $\times$ , 150 $\times$ ) result in decreased performance. However, for EuroSAT, an accuracy of around 98.6% is achieved at 10 $\times$ , with lower and higher rates underperforming. These findings demonstrate that while a substantial increase in the learning rate from pre-training is generally beneficial, the optimal rate can vary significantly depending on the specific dataset.

## V. CONCLUSION

In this work, we introduced SVFit, a novel PEFT method that enhances initialization by leveraging SVD to initialize

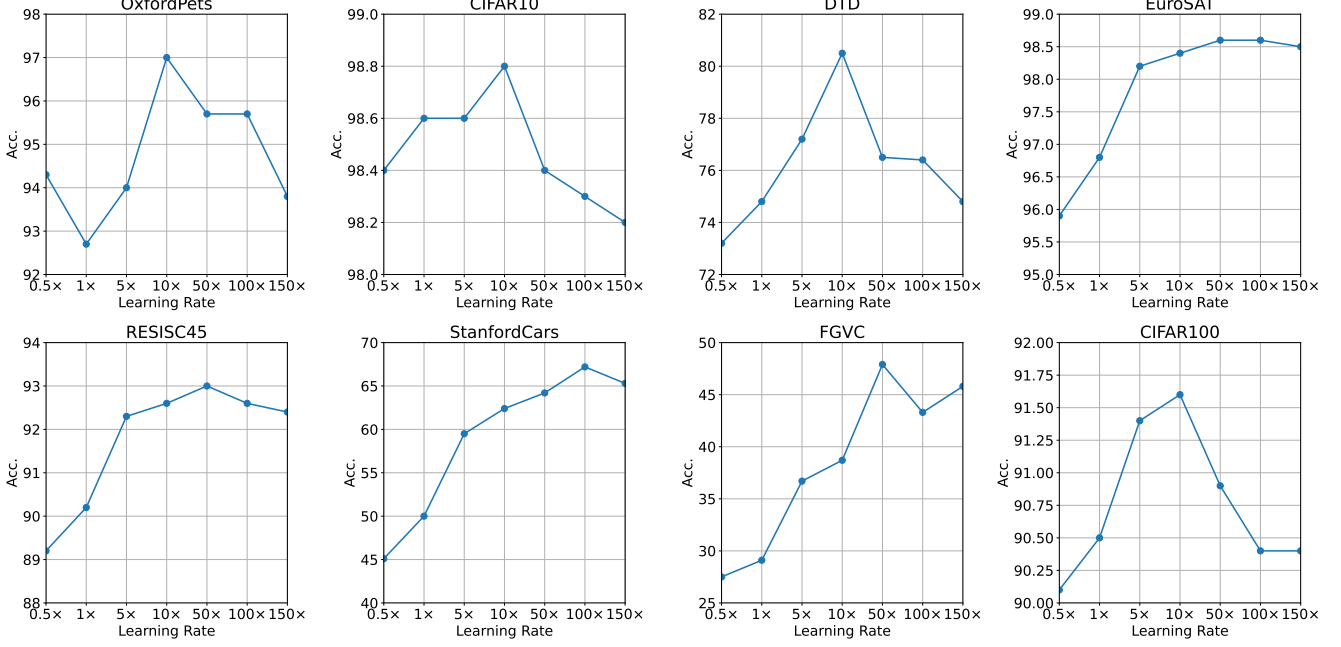


Fig. 6. Performance of SVFit fine-tuning for ViT-base model on image classification tasks across different learning rate. The  $x$ -axis represents the learning rate, and the  $y$ -axis is the evaluation index of different datasets.

low-rank matrices derived from pre-trained weights. SVFit focuses on training only the most significant top- $r$  singular values, significantly reducing the number of trainable parameters while ensuring efficient fine-tuning and preserving the model’s core capabilities. Our theoretical analysis demonstrates how this approach enables rapid adaptation by effectively capturing essential information from pre-trained models and efficiently learning new domain-specific knowledge with minimal parameters. SVFit has been evaluated across various tasks, including natural language understanding, image classification, and subject-driven text-to-image generation, consistently outperforming LoRA and other recent state-of-the-art techniques such as PiSSA in both efficiency and effectiveness. Future work will focus on extending SVFit to more complex tasks, optimizing singular value selection, and further enhancing performance through dynamic parameter budget allocation to broaden its applicability across diverse domains.

#### ACKNOWLEDGEMENTS

This research was partially funded by the National Natural Science Foundation of China under grants 62220106008, 62306067, and U20B2063, as well as the Sichuan Science and Technology Program under grant 2024NSFSC1463. Additional support was provided by the Sichuan Province Innovative Talent Funding Project for Postdoctoral Fellows (Project BX202311) and the China Postdoctoral Science Foundation (Project 2022M720660).

#### REFERENCES

- [1] Y. Liu, M. Ott, N. Goyal, J. Du, M. Joshi, D. Chen, O. Levy, M. Lewis, L. Zettlemoyer, and V. Stoyanov, “Roberta: A robustly optimized bert pretraining approach,” *arXiv:1907.11692*, 2019.
- [2] A. Dosovitskiy, L. Beyer, A. Kolesnikov, D. Weissenborn, X. Zhai, T. Unterthiner, M. Dehghani, M. Minderer, G. Heigold, S. Gelly *et al.*, “An image is worth 16x16 words: Transformers for image recognition at scale,” in *International Conference on Learning Representations, ICLR*, 2021.
- [3] H. Touvron, L. Martin, K. Stone, P. Albert, A. Almahairi, Y. Babaei, N. Bashlykov, S. Batra, P. Bhargava, S. Bhosale *et al.*, “Llama 2: Open foundation and fine-tuned chat models,” *arXiv:2307.09288*, 2023.
- [4] C. Raffel, N. Shazeer, A. Roberts, K. Lee, S. Narang, M. Matena, Y. Zhou, W. Li, and P. J. Liu, “Exploring the limits of transfer learning with a unified text-to-text transformer,” *J Mach Learn Res*, vol. 21, no. 140, pp. 1–67, 2020.
- [5] J. Devlin, M.-W. Chang, K. Lee, and K. Toutanova, “Bert: Pre-training of deep bidirectional transformers for language understanding,” *arXiv:1810.04805*, 2018.
- [6] A. Radford, J. Wu, R. Child, D. Luan, D. Amodei, I. Sutskever *et al.*, “Language models are unsupervised multitask learners,” *OpenAI blog*, vol. 1, no. 8, p. 9, 2019.
- [7] L. Yuan, Y. Chen, T. Wang, W. Yu, Y. Shi, Z.-H. Jiang, F. E. Tay, J. Feng, and S. Yan, “Tokens-to-token vit: Training vision transformers from scratch on imagenet,” in *IEEE International Conference on Computer Vision, ICCV*, 2021, pp. 558–567.
- [8] D. Zhou, B. Kang, X. Jin, L. Yang, X. Lian, Z. Jiang, Q. Hou, and J. Feng, “Deepvit: Towards deeper vision transformer,” *arXiv:2103.11886*, 2021.
- [9] H. Zhao, L. Jiang, J. Jia, P. H. Torr, and V. Koltun, “Point transformer,” in *IEEE International Conference on Computer Vision, ICCV*, 2021, pp. 16 259–16 268.
- [10] J. Wei, Y. Yang, X. Xu, J. Song, G. Wang, and H. T. Shen, “Less is better: Exponential loss for cross-modal matching,” *IEEE Trans. Circuits Syst. Video Technol.*, vol. 33, no. 9, pp. 5271–5280, 2023.
- [11] Z.-Y. Wang, X. P. Li, H. C. So, and A. M. Zoubir, “Adaptive rank-one matrix completion using sum of outer products,” *IEEE Trans. Circuits Syst. Video Technol.*, vol. 33, no. 9, pp. 4868–4880, 2023.
- [12] W. Yan, M. Yang, and Y. Li, “Robust low rank and sparse representation for multiple kernel dimensionality reduction,” *IEEE Trans. Circuits Syst. Video Technol.*, vol. 33, no. 1, pp. 1–15, 2023.
- [13] Y. Xu, J. Wei, Y. Bin, Y. Yang, Z. Ma, and H. T. Shen, “Set of diverse queries with uncertainty regularization for composed image retrieval,” *IEEE Trans. Circuits Syst. Video Technol.*, pp. 1–1, 2024.
- [14] S. Kim, I. Kang, and N. Kwak, “Semantic sentence matching with densely-connected recurrent and co-attentive information,” in *Proceed-*

ings of the AAAI conference on artificial intelligence, AAAI, vol. 33, no. 01, 2019, pp. 6586–6593.

[15] L. Ouyang, J. Wu, X. Jiang, D. Almeida, C. Wainwright, P. Mishkin, C. Zhang, S. Agarwal, K. Slama, A. Ray *et al.*, “Training language models to follow instructions with human feedback,” *Advances in neural information processing systems, NeurIPS*, vol. 35, pp. 27730–27744, 2022.

[16] K. Hambardzumyan, H. Khachatrian, and J. May, “Warp: Word-level adversarial reprogramming,” *arXiv:2101.00121*, 2021.

[17] T. Wolf, L. Debut, V. Sanh, J. Chaumond, C. Delangue, A. Moi, P. Cistac, T. Rault, R. Louf, M. Funtowicz *et al.*, “Transformers: State-of-the-art natural language processing,” in *Conference on Empirical Methods in Natural Language Processing, EMNLP*, 2020, pp. 38–45.

[18] N. Ding, Y. Qin, G. Yang, F. Wei, Z. Yang, Y. Su, S. Hu, Y. Chen, C.-M. Chan, W. Chen *et al.*, “Parameter-efficient fine-tuning of large-scale pre-trained language models,” *Nat. Mach. Intell.*, vol. 5, no. 3, pp. 220–235, 2023.

[19] E. J. Hu, Y. Shen, P. Wallis, Z. Allen-Zhu, Y. Li, S. Wang, L. Wang, and W. Chen, “Lora: Low-rank adaptation of large language models,” in *International Conference on Learning Representations, ICLR*, 2022.

[20] B. Zi, X. Qi, L. Wang, J. Wang, K.-F. Wong, and L. Zhang, “Delta-lora: Fine-tuning high-rank parameters with the delta of low-rank matrices,” *arXiv:2309.02411*, 2023.

[21] D. J. Kopczko, T. Blankevoort, and Y. M. Asano, “Vera: Vector-based random matrix adaptation,” in *International Conference on Learning Representations, ICLR*, 2024.

[22] Y. Gu, X. Han, Z. Liu, and M. Huang, “Ppt: Pre-trained prompt tuning for few-shot learning,” in *Annual Meeting of the Association for Computational Linguistics, ACL*, 2022, pp. 8410–8423.

[23] P. Ren, C. Shi, S. Wu, M. Zhang, Z. Ren, M. de Rijke, Z. Chen, and J. Pei, “Mini-ensemble low-rank adapters for parameter-efficient fine-tuning,” *arXiv:2402.17263*, 2024.

[24] M. Valipour, M. Rezagholizadeh, I. Kobyzev, and A. Ghodsi, “Dylora: Parameter efficient tuning of pre-trained models using dynamic search-free low-rank adaptation,” *arXiv:2210.07558*, 2022.

[25] S.-A. Rebuffi, H. Bilen, and A. Vedaldi, “Learning multiple visual domains with residual adapters,” *Advances in neural information processing systems, NeurIPS*, vol. 30, pp. 506–516, 2017.

[26] X. L. Li and P. Liang, “Prefix-tuning: Optimizing continuous prompts for generation,” in *Annual Meeting of the Association for Computational Linguistics, ACL*, 2021.

[27] B. Lester, R. Al-Rfou, and N. Constant, “The power of scale for parameter-efficient prompt tuning,” in *Conference on Empirical Methods in Natural Language Processing, EMNLP*, 2021, pp. 3045–3059.

[28] C. Li, H. Farkhoor, R. Liu, and J. Yosinski, “Measuring the intrinsic dimension of objective landscapes,” *arXiv:1804.08838*, 2018.

[29] L. Zhang, L. Zhang, S. Shi, X. Chu, and B. Li, “Lora-fa: Memory-efficient low-rank adaptation for large language models fine-tuning,” *arXiv:2308.03303*, 2023.

[30] V. Ramanujan, M. Wortsman, A. Kembhavi, A. Farhadi, and M. Rastegari, “What’s hidden in a randomly weighted neural network?” in *IEEE Conference on Computer Vision and Pattern Recognition, CVPR*, 2020, pp. 11893–11902.

[31] K. Zhang, W. Zuo, Y. Chen, D. Meng, and L. Zhang, “Beyond a gaussian denoiser: Residual learning of deep cnn for image denoising,” *IEEE Trans. Image Process.*, vol. 26, no. 7, pp. 3142–3155, 2017.

[32] E. Xie, L. Yao, H. Shi, Z. Liu, D. Zhou, Z. Liu, J. Li, and Z. Li, “Diffit: Unlocking transferability of large diffusion models via simple parameter-efficient fine-tuning,” in *IEEE International Conference on Computer Vision, ICCV*, 2023, pp. 4230–4249.

[33] T. Brown, B. Mann, N. Ryder, M. Subbiah, J. D. Kaplan, P. Dhariwal, A. Neelakantan, P. Shyam, G. Sastry, A. Askell *et al.*, “Language models are few-shot learners,” in *Advances in Neural Information Processing Systems, NeurIPS*, vol. 33, 2020, pp. 1877–1901.

[34] H. Touvron, L. Martin, K. Stone, P. Albert, A. Almahairi, Y. Babaei, N. Bashlykov, S. Batra, P. Bhargava, S. Bhosale *et al.*, “Llama 2: Open foundation and fine-tuned chat models,” *arXiv:2307.09288*, 2023.

[35] J. Wei, M. Bosma, V. Y. Zhao, K. Guu, A. W. Yu, B. Lester, N. Du, A. M. Dai, and Q. V. Le, “Finetuned language models are zero-shot learners,” *arXiv:2109.01652*, 2021.

[36] A. Vaswani, N. Shazeer, N. Parmar, J. Uszkoreit, L. Jones, A. N. Gomez, Ł. Kaiser, and I. Polosukhin, “Attention is all you need,” in *Advances in neural information processing systems, NeurIPS*, 2017.

[37] Z. Lin, A. Madotto, and P. Fung, “Exploring versatile generative language model via parameter-efficient transfer learning,” in *Conference on Empirical Methods in Natural Language Processing, EMNLP*, 2020, pp. 441–459.

[38] F. Meng, Z. Wang, and M. Zhang, “Pissa: Principal singular values and singular vectors adaptation of large language models,” *arXiv:2404.02948*, 2024.

[39] Q. Zhang, M. Chen, A. Bukharin, N. Karampatziakis, P. He, Y. Cheng, W. Chen, and T. Zhao, “Adaptive budget allocation for parameter-efficient fine-tuning,” in *International Conference on Learning Representations, ICLR*, 2023.

[40] N. Ding, X. Lv, Q. Wang, Y. Chen, B. Zhou, Z. Liu, and M. Sun, “Sparse low-rank adaptation of pre-trained language models,” *arXiv:2311.11696*, 2023.

[41] F. Zhang, L. Li, J. Chen, Z. Jiang, B. Wang, and Y. Qian, “Increlora: Incremental parameter allocation method for parameter-efficient fine-tuning,” *arXiv:2308.12043*, 2023.

[42] C.-W. Sun, T.-Z. Huang, T. Xu, and L.-J. Deng, “Nf-3dlogtnn: An effective hyperspectral and multispectral image fusion method based on nonlocal low-fibered-rank regularization,” *Appl. Math. Model.*, vol. 118, pp. 780–797, 2023.

[43] T. Xu, T.-Z. Huang, L.-J. Deng, and N. Yokoya, “An iterative regularization method based on tensor subspace representation for hyperspectral image super-resolution,” *IEEE Trans. Geosci. Remote Sens.*, vol. 60, pp. 1–16, 2022.

[44] N. Halko, P.-G. Martinsson, and J. A. Tropp, “Finding structure with randomness: Probabilistic algorithms for constructing approximate matrix decompositions,” *Siam Rev.*, vol. 53, no. 2, pp. 217–288, 2011.

[45] A. G. Akritas and G. I. Malaschonok, “Applications of singular-value decomposition (svd),” *Math. Comput. Simul.*, vol. 67, no. 1-2, pp. 15–31, 2004.

[46] A. Wang, A. Singh, J. Michael, F. Hill, O. Levy, and S. R. Bowman, “Glue: A multi-task benchmark and analysis platform for natural language understanding,” in *International Conference on Learning Representations, ICLR*, 2019.

[47] T. Su, D. Feng, M. Wang, and M. Chen, “Dual discriminative low-rank projection learning for robust image classification,” *IEEE Trans. Circuits Syst. Video Technol.*, vol. 33, no. 12, pp. 7708–7722, 2023.

[48] H. Liu, Y. Jia, J. Hou, and Q. Zhang, “Global-local balanced low-rank approximation of hyperspectral images for classification,” *IEEE Trans. Circuits Syst. Video Technol.*, vol. 32, no. 4, pp. 2013–2024, 2022.

[49] R. Rombach, A. Blattmann, D. Lorenz, P. Esser, and B. Ommer, “High-resolution image synthesis with latent diffusion models,” in *IEEE Conference on Computer Vision and Pattern Recognition, CVPR*, 2022, pp. 10684–10695.

[50] R. Gal, Y. Alaluf, Y. Atzmon, O. Patashnik, A. H. Bermano, G. Chechik, and D. Cohen-Or, “An image is worth one word: Personalizing text-to-image generation using textual inversion,” *arXiv:2208.01618*, 2022.

[51] N. Ruiz, Y. Li, V. Jampani, Y. Pritch, M. Rubinstein, and K. Aberman, “Dreambooth: Fine tuning text-to-image diffusion models for subject-driven generation,” in *IEEE Conference on Computer Vision and Pattern Recognition, CVPR*, 2023, pp. 22500–22510.

[52] T. Wolf, L. Debut, V. Sanh, J. Chaumond, C. Delangue, A. Moi, P. Cistac, T. Rault, R. Louf, M. Funtowicz *et al.*, “Huggingface’s transformers: State-of-the-art natural language processing,” *arXiv:1910.03771*, 2019.

[53] S. Huang, D. Xu, I. E. Yen, Y. Wang, S.-E. Chang, B. Li, S. Chen, M. Xie, S. Rajasekaran, H. Liu *et al.*, “Sparse progressive distillation: Resolving overfitting under pretrain-and-finetune paradigm,” in *Annual Meeting of the Association for Computational Linguistics, ACL*, 2022.

[54] A. Warstadt, A. Singh, and S. R. Bowman, “Neural network acceptability judgments,” *Trans. Assoc. Comput. Linguist.*, vol. 7, pp. 625–641, 2019.

[55] D. Cer, M. Diab, E. Agirre, I. Lopez-Gazpio, and L. Specia, “Semeval-2017 task 1: Semantic textual similarity-multilingual and cross-lingual focused evaluation,” *arXiv:1708.00055*, 2017.

[56] D. Giampiccolo, B. Magnini, I. Dagan, and W. B. Dolan, “The third pascal recognizing textual entailment challenge,” in *Proceedings of the ACL-PASCAL workshop on textual entailment and paraphrasing*, 2007, pp. 1–9.

[57] B. Dolan and C. Brockett, “Automatically constructing a corpus of sentential paraphrases,” in *Third international workshop on paraphrasing (IWP2005)*, 2005.

[58] R. Socher, A. Perelygin, J. Wu, J. Chuang, C. D. Manning, A. Y. Ng, and C. Potts, “Recursive deep models for semantic compositionality over a sentiment treebank,” in *Conference on Empirical Methods in Natural Language Processing, EMNLP*, 2013, pp. 1631–1642.

[59] P. Rajpurkar, J. Zhang, K. Lopyrev, and P. Liang, “Squad: 100,000+ questions for machine comprehension of text,” in *Conference on Empirical Methods in Natural Language Processing, EMNLP*, 2016, pp. 2383–2392.

- [60] Z. Gao, Q. Wang, A. Chen, Z. Liu, B. Wu, L. Chen, and J. Li, “Parameter-efficient fine-tuning with discrete fourier transform,” *arXiv:2405.03003*, 2024.
- [61] T. Ridnik, E. Ben-Baruch, A. Noy, and L. Zelnik-Manor, “Imagenet-21k pretraining for the masses,” *arXiv:2104.10972*, 2021.
- [62] O. M. Parkhi, A. Vedaldi, A. Zisserman, and C. Jawahar, “Cats and dogs,” in *IEEE Conference on Computer Vision and Pattern Recognition, CVPR*, 2012, pp. 3498–3505.
- [63] A. Krizhevsky, G. Hinton *et al.*, “Learning multiple layers of features from tiny images,” *Master’s thesis, University of Tront*, 2009.
- [64] M. Cimpoi, S. Maji, I. Kokkinos, S. Mohamed, and A. Vedaldi, “Describing textures in the wild,” in *IEEE Conference on Computer Vision and Pattern Recognition, CVPR*, 2014, pp. 3606–3613.
- [65] P. Helber, B. Bischke, A. Dengel, and D. Borth, “Eurosat: A novel dataset and deep learning benchmark for land use and land cover classification,” *IEEE J. Sel. Top. Appl. Earth Observ. Remote Sens.*, vol. 12, no. 7, pp. 2217–2226, 2019.
- [66] G. Cheng, J. Han, and X. Lu, “Remote sensing image scene classification: Benchmark and state of the art,” *Proceedings of the IEEE*, vol. 105, no. 10, pp. 1865–1883, 2017.
- [67] J. Krause, M. Stark, J. Deng, and L. Fei-Fei, “3d object representations for fine-grained categorization,” in *IEEE International Conference on Computer Vision, ICCV*, 2013, pp. 554–561.
- [68] S. Maji, E. Rahtu, J. Kannala, M. Blaschko, and A. Vedaldi, “Fine-grained visual classification of aircraft,” *arXiv:1306.5151*, 2013.